

Studies on track quality at the ZEUS detector and HERA beamspot size determination

Summer Student Program 2009, DESY

Alexandru Dafinca

University of Oxford

supervised by Olaf Behnke

September 2009

Abstract

The ZEUS micro vertex detector (MVD) has been recalibrated for the final data analysis of the HERA II data. The aim of this project is a detailed check of the achieved spatial resolution of the tracks close to the ep primary vertex region. This resolution is essential for all charm and beauty quark production analyses which rely on lifetime tagging. An attempt has been made at disentangling the intrinsic resolution of the detector from the beamspot size effect and the effect of multiple scattering. For this a study of the beamspot size and how it varies from HERA period to period has been performed and the combined effect of the intrinsic detector resolution and multiple scattering has been determined for different values of the transverse momentum.

Contents

1	Physics motivation	3
2	Basics of track quality	4
3	HERA beamspot size in the ZEUS detector	5
3.1	Theory	5
3.2	Cuts on data	10
3.3	Results - beamspot size at HERA between 2003 and 2007	10
4	Multiple Scattering and Intrinsic Resolution	11
4.1	Resolution of the impact parameter in different scenarios	11
4.2	Cuts on data	14
4.3	Results	14
4.3.1	Comparison of σ_{IP} and $\sigma_{MS} \oplus \sigma_{IR}$ for fixed $p_t = 5\text{GeV} \pm 10\%$ (figure 15)	14
4.3.2	Comparison of $\sigma_{MS} \oplus \sigma_{IR}$ for $p_t = 5\text{GeV} \pm 10\%$ and $p_t = 2\text{GeV} \pm 10\%$ (figure 16)	15
4.3.3	Comparison of $\sigma_{MS} \oplus \sigma_{IR}$ for $p_t = 5\text{GeV} \pm 10\%$ for real data and Monte Carlo data (figure 17)	16
5	Conclusions	16
6	Acknowledgements	17

1 Physics motivation

This work was performed in order to improve the measurements of charm and beauty quark production with the HERA II data. The main production mechanism for these heavy quarks is shown in figure 1. This process allows to obtain direct information on the gluon density in the proton, since it is closely related to the cross-section for production of charmed and beautiful quarks. In order to measure this cross-section one first needs to identify the events containing charm or beauty quarks, which can be done thanks to the typical signatures. In figure 2 we show such a typical signature resulting from the long lifetime of the D^+ ($c\bar{b}$) meson which decays electroweakly.

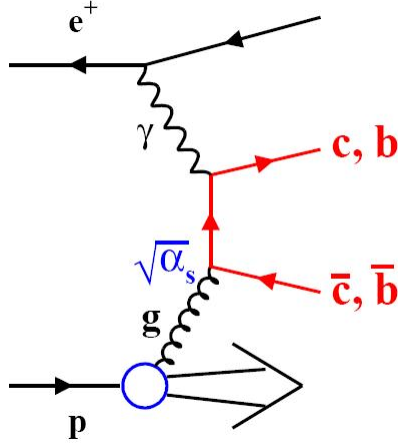


Figure 1: Main production diagram for charm and beauty quarks in ep collisions at HERA. (diagram Olaf Behnke)

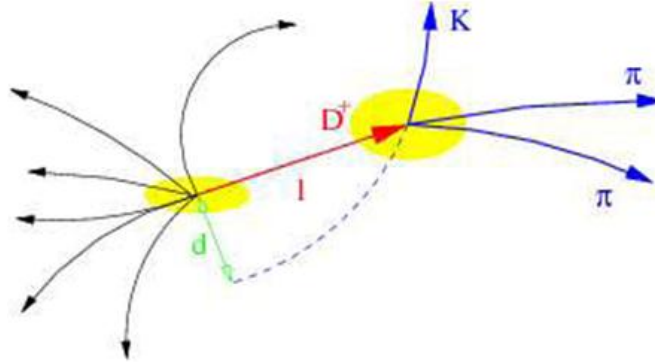


Figure 2: Sketch of D^+ meson production and subsequent decay in three charged particles. On the right hand side the reconstruction of such a candidate event is shown, where one can see (in the transverse plane) the tracks as they are measured in the ZEUS barrel micro vertex detector (BMVD). (diagram Olaf Behnke)

Before it does so, it typically flies a few 100 μm in the detector. The secondary vertex (position of the D^+ decay) can be reconstructed from the charged decay tracks if they are measured precisely enough. This is the task of the BMVD (Barrel Microvertex Detector). This detector consists of three layers of silicon strip detectors, placed just around the beampipe, very close to the interaction

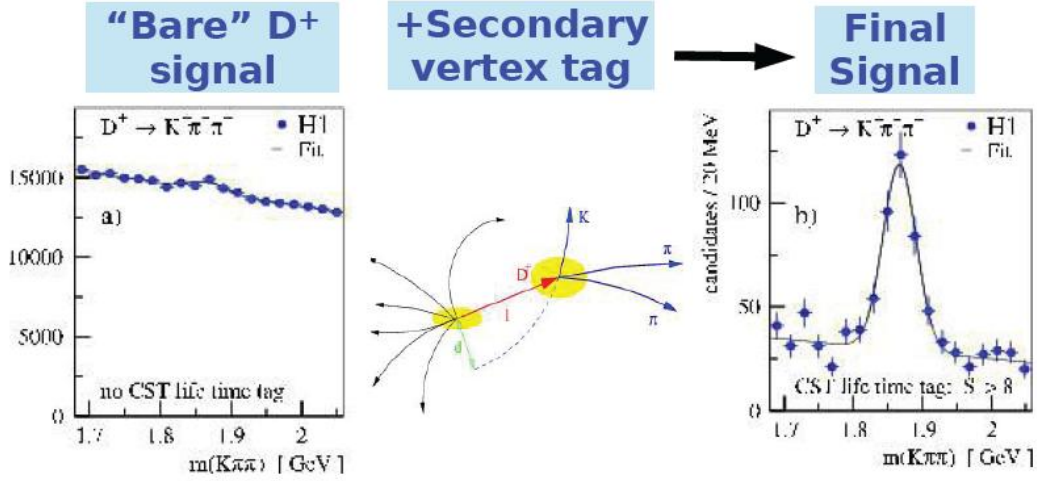


Figure 3: Improvement of D^+ signal through secondary vertex tagging (plots and diagram provided by Olaf Behnke, taken from the H1 analysis DESY-04-156)

point. There are in total 30 ladders, each containing 10 $r\phi$ and 10 z sensors. For the former ones the strips are parallel to the z -axis (which is parallel to the proton beam) and for the latter one perpendicular. In each sensor the position of a track passing through can be measured with a precision of about 20 μm .

Why do we need such high precision? If the tracks were reconstructed with a large error, it would be impossible to tell apart the primary vertex from the secondary vertex and thus all particles would seem to be flying off from the same interaction point - the typical signature of D^+ would be washed out. However, if the tracks were reconstructed with a small uncertainty, one could distinguish very well the two vertices and would recognize that there must have been a particle flying from one vertex to the other - the D^+ is detected! But how far away do the vertices need to be in order to be sure they are distinct points and not the same?

In figure 3 the invariant mass of the particles expected to fly off from the secondary vertex has been built ($K\pi\pi$). On the right hand side we present the same plot but with the following cut. We only accept the events for which the distance between the reconstructed vertices (the red arrow) is at least 8 times larger than the combined error of the individual reconstructed vertices (represented by the yellow blobs). The final signal exhibits a clear peak at the D^+ mass.

In order for this analysis to work we need to know the errors in the positions of the reconstructed vertices and thus the errors in the reconstructed tracks. If we impose too severe conditions on the decay length of the D^+ , the statistics will be drastically reduced - an accurate knowledge of the resolution of the tracks is crucial in order to not lose too much of the signal.

2 Basics of track quality

A metric of track quality is desirable for this study - the aim of this section is to introduce the reader to some well-established definitions.

In the ideal case, the beamspot ($r\phi$ - cross section of the beam) is just a mathematical point. The reconstructed track passes through the beamspot. Excellent. In real life however, things are more complicated. First of all, the beamspot is not a point, but an ellipse. Secondly, the

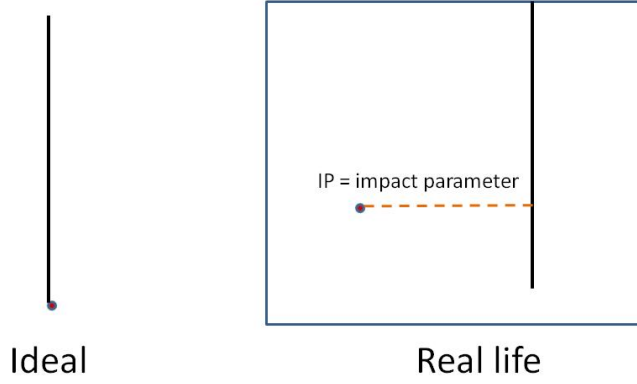


Figure 4: Impact parameter - ideal vs. real life

reconstructed track does not pass through the center of the beamspot, often not even through the beamspot. The shortest distance from the track to the beam, as depicted in figure 4, is called an impact parameter. The following convention has been used for the sign of the impact parameter:

$$\text{Sgn}(IP) \equiv \text{Sgn}\left(\frac{\mathbf{r} \times \mathbf{p}}{|\mathbf{r} \times \mathbf{p}|}\right)$$

which is basically the sign of the projection of the angular momentum of the particle associated with the track on the z - axis.

There are mainly three effects which are responsible for the emergence of an impact parameter:

- multiple scattering (fig. 5) - describes the interaction of a particle with the beampipe and/or the detector by which the particle gets deflected from its original path. However, we only have detectors outside the beampipe - they will reconstruct the track without knowing about the real path of the particle within the beampipe. Therefore, even though the particle comes from the beamspot, to the detector it looks as if it came from a point some distance away from the beamspot. A detailed account on this process can be found in [1].
- the intrinsic resolution of the detector - the hits in the detector are close to, but not the same as the points through which a particle actually flew. This introduces an uncertainty in the reconstruction of the track, such that the reconstructed track will not hit the beamspot.
- size of the beamspot - the beamspot is not a mathematical point, but an ellipse. This means that the actual interaction can take place anywhere within this ellipse. Even if the tracks are reconstructed perfectly, since the interaction point and the beamspot center are not the same, the tracks will have an impact parameter associated with them.

The approximate sizes of these effects can be seen in figure 6. It is important to notice that the multiple scattering effect is dependent on the transverse momentum p_t ; for high $p_t \gtrsim 5\text{GeV}$, the multiple scattering effect is negligible.

3 HERA beamspot size in the ZEUS detector

3.1 Theory

Knowing precisely the size of the beamspot is advantageously when disentagling the three different effects affecting the resolution of the tracks. A very elegant method can be used, involving

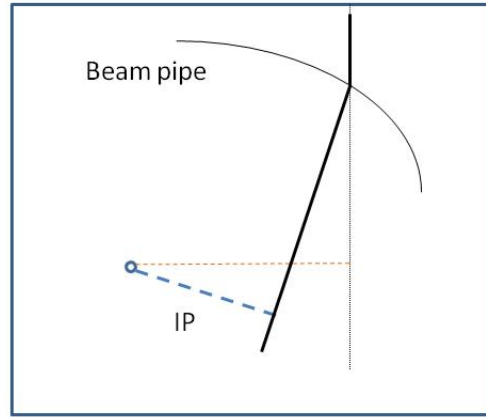


Figure 5: Effect of multiple scattering on the impact parameter

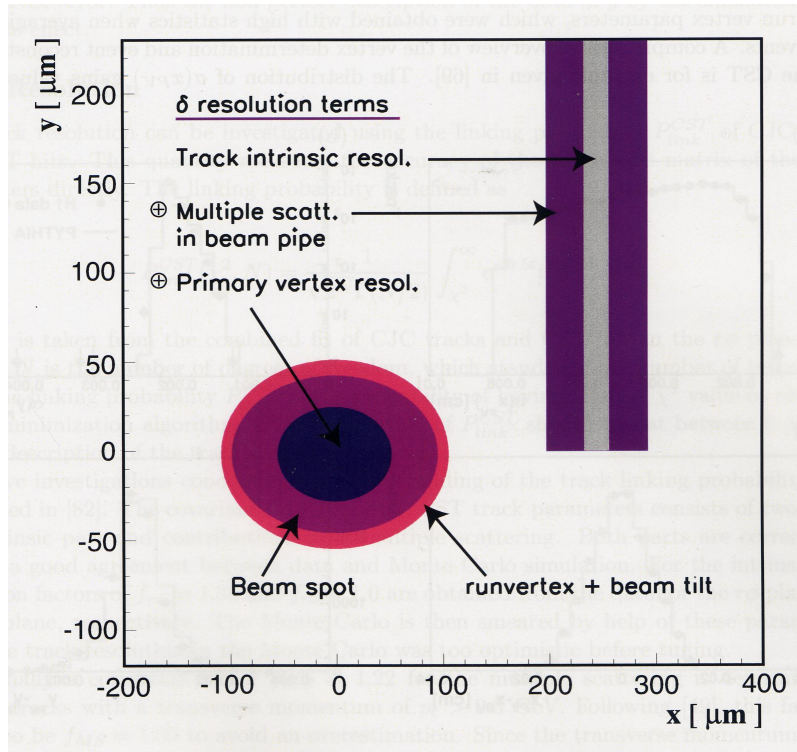


Figure 6: Contributions to the track resolution (schematic diagram - Olaf Behnke)

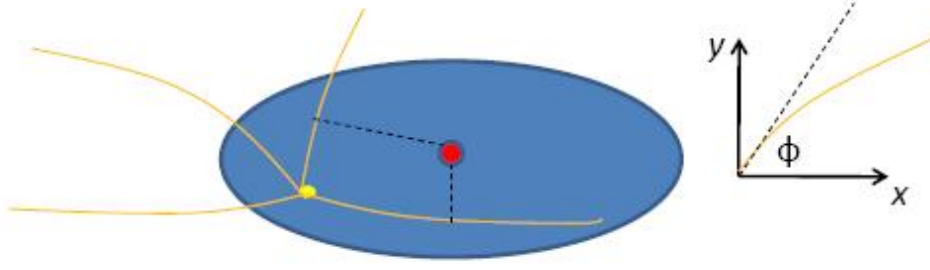


Figure 7: Sketch of the beamspot

track-track impact parameter correlations. There are several others, using for example a method designed by Olaf Behnke, where very well reconstructed primary vertices with many tracks are used. Information on the beamspot size is also available from the machine beam optics itself, but an independent measurement in the detector is desirable.

Assume the intrinsic resolution of tracks is perfect and there is no multiple scattering. (Eventually the effect of these two would be to change the errors with which we determine the size of the beamspot; however, the determined size of the beamspot itself would not change - i.e. the precision is altered, but not the accuracy.) Consider an interaction somewhere within the beamspot (figure 3.1). We assume particles are flying off from the interaction point. Let us look at two tracks where the particles fly off at certain angles ϕ_1 and ϕ_2 . Build the product $IP_1 \cdot IP_2$. Now loop through all events and look for other pairs of tracks with exactly the same angles and compute the same product as before. Eventually build the average $\langle IP_1 \cdot IP_2 \rangle$. Rainer Mankel showed ([2]) that this average depends in a fortuituous way on the size of the beamspot:

$$\langle IP_1 \cdot IP_2 \rangle = \sigma_x^2 \cdot \sin \phi_1 \cdot \sin \phi_2 + \sigma_y^2 \cdot \cos \phi_1 \cdot \cos \phi_2 \quad (1)$$

The plan of attack is obvious now: we compute the average $\langle IP_1 \cdot IP_2 \rangle$ for different combinations of the two angles ϕ_1 and ϕ_2 , exploring the whole $\phi_1 - \phi_2$ space (like in figure 9) and fit the above function (1) to the data. Through the fit the two free parameters σ_x and σ_y can be determined.

We show the data and the fit to it exemplarily for the 2005e sample. A decent fit with $\chi^2/\text{d.o.f.} = 4.44$ was found. If we build the ratio of data to the fitted function (figure 10), we would have in the ideal case a ratio equal to 1. The “cross” structure in the plot of the ratio emerges due to the fact that on the cross the fitted function is exactly or very close to 0. Even though the *absolute* difference between fit function and data might be the same everywhere, on the cross the *relative* error will be much larger.

Therefore we also present in figure 11 the difference between real data and fitted function. The agreement is fairly good, however we recognize again some structure. This suggests that there are still errors in our assumptions that need to be corrected for. One of the possible reasons for the discrepancy is that in this analysis we might have included tracks that actually come from a secondary vertex but have been wrongly fitted to a primary vertex. These can be filtered out by imposing a more severe cut on p_t . Another possible reason is some small residual misalignment of the BMVD detector.

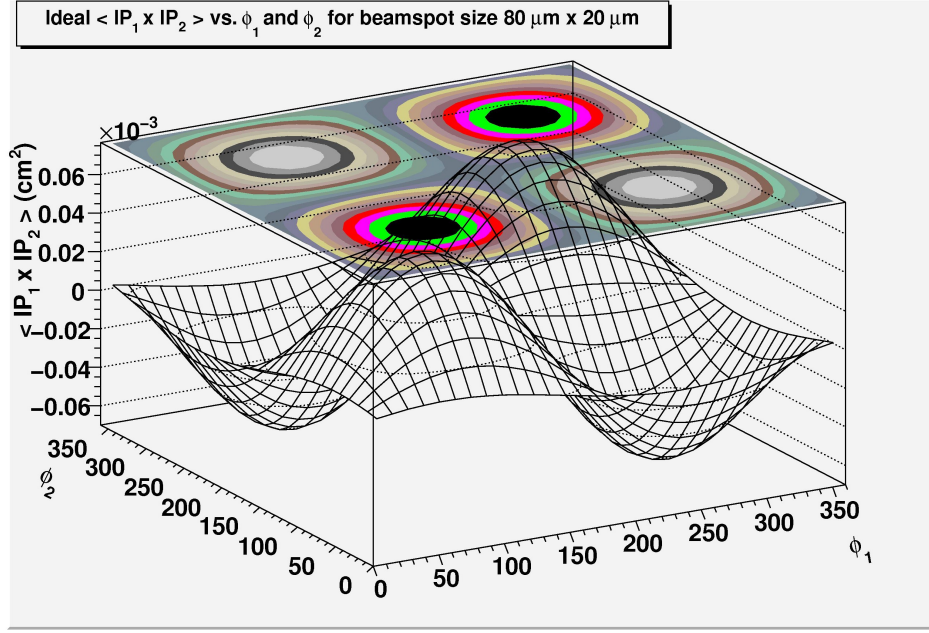


Figure 8: Ideal $\langle IP_1 \cdot IP_2 \rangle$ as a function of ϕ_1 and ϕ_2 for a beamspot with $\sigma_x = 80\mu\text{m}$ and $\sigma_y = 20\mu\text{m}$

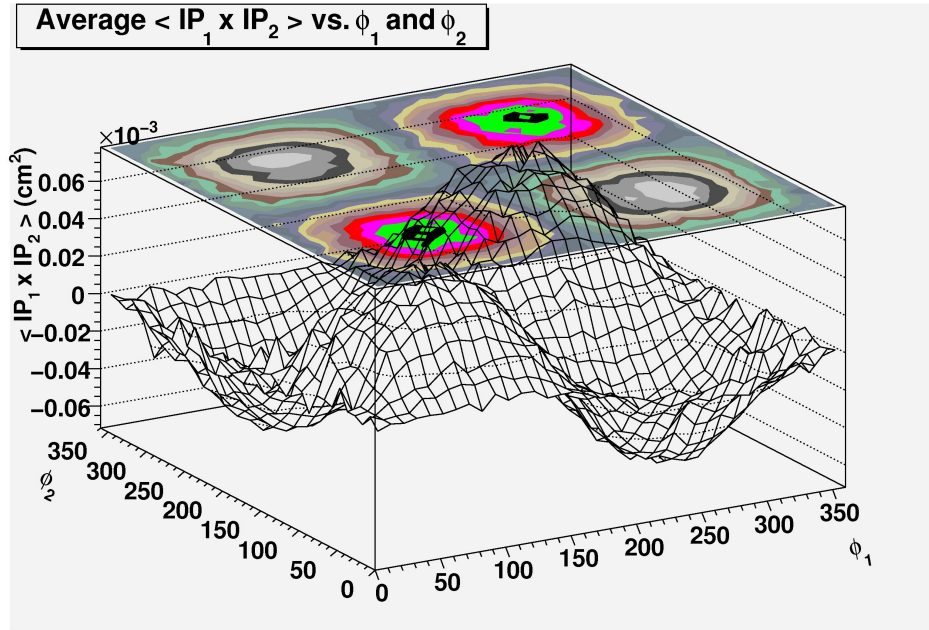


Figure 9: $\langle IP_1 \cdot IP_2 \rangle$ for different combinations of the two angles ϕ_1 and ϕ_2 in the case of the 05e data.

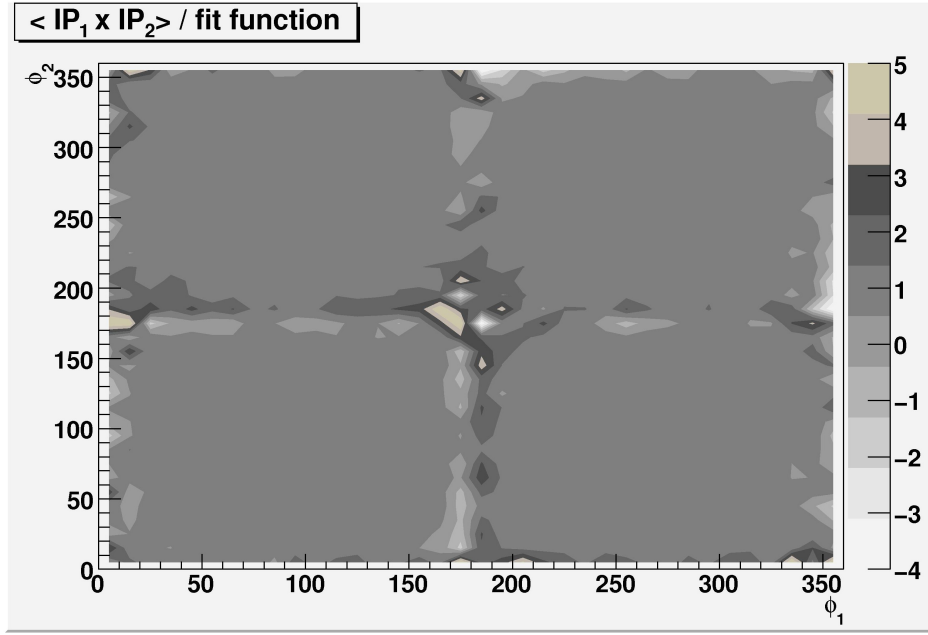


Figure 10: Ratio $\langle IP_1 \cdot IP_2 \rangle / \text{fitted function}$ for the determination of the beamspot size

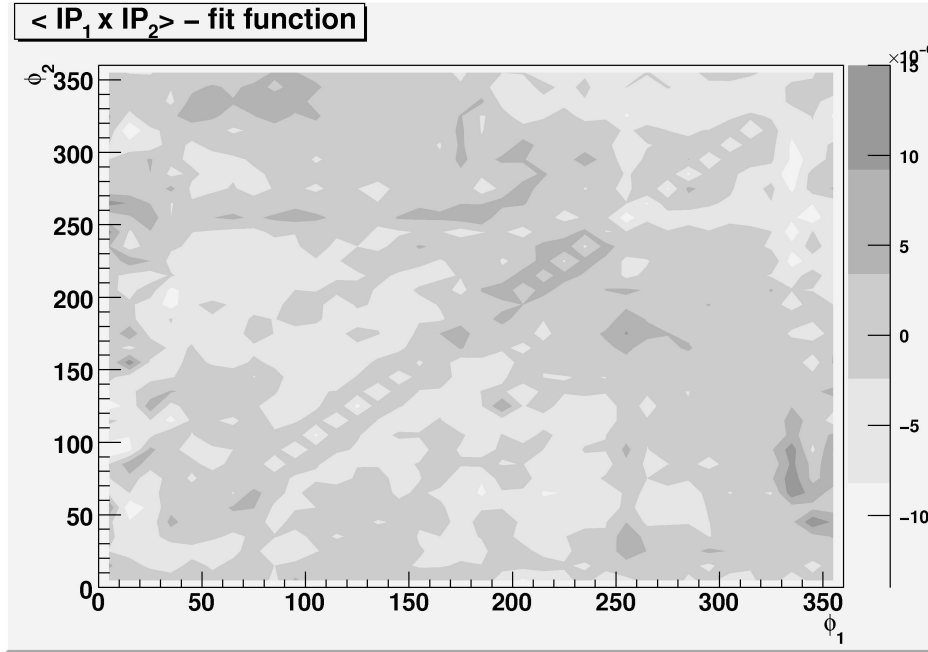


Figure 11: Difference between real data and the fitted function for the determination of the beamspot size

Sample	Runnr.	No. of events	No. of good track pairs	$\sigma_x(\mu\text{m})$	$\sigma_y(\mu\text{m})$	$\chi^2/\text{d.o.f}$
03p	45783 - 46596	3 705 000	333 690	82.90 ± 0.35	13.07 ± 2.82	1.17
04p	47010 - 51245	47 468 000	4 956 854	86.88 ± 0.09	16.31 ± 0.60	3.63
05e	52258 - 57123	123 521 000	20 159 200	78.59 ± 0.05	8.04 ± 0.62	4.44
06e	58207 - 59947	44 069 000	8 201 224	77.75 ± 0.07	8.67 ± 0.87	2.29
06p	60005 - 61746	86 514 000	1 346 437	86.78 ± 0.05	15.97 ± 0.38	3.51
07p	61747 - 62636	40 972 000	5 927 484	84.95 ± 0.08	15.61 ± 0.59	1.20
07 low	70000 - 70818	20 986 000	1 421 239	136.51 ± 0.15	40.64 ± 0.55	3.96
07 mid	71004 - 71401	8 805 000	618 671	119.21 ± 0.24	34.50 ± 0.91	1.73
MC1	*see footnote	1 000 000	613 437	78.10 ± 0.25	16.30 ± 1.57	1.32
MC2	*see footnote	7 079 477	3 684 149	78.57 ± 0.10	19.29 ± 0.55	2.09

Table 1: Beamspot size for the different run periods at HERA between 2003 and 2007. p stands for positron - proton collisions, e stands for electron - proton collisions. 07 low and 07 mid are low energy respectively mid-energy runs. MC stands for Monte Carlo simulations. MC1 is a subset of the MC2 sample.

3.2 Cuts on data

We only look at events occuring at a primary vertex, where:

- the absolute value of the z coordinate of the vertex is < 20 cm
- there are at 10 or more tracks fitted to the same vertex
- EVTAKE = 1

Further, we require each track to:

- have 2 or more hits in each projection in the MVD
- outer SuperLayer = 9
- transverse momentum $p_t > 1\text{GeV}$

3.3 Results - beamspot size at HERA between 2003 and 2007¹

The results of this analysis have been summarized in table 1 and figure 12.

MC2 is the same data as MC1 + about 6 million more events.² The MC data has been produced by assuming a beamspot size with the parameters $\sigma_x = 80\mu\text{m}$ and $\sigma_y = 20\mu\text{m}$. While the fitted σ_x and σ_y for MC2 are in good accordance with the nominal values, we can identify a bias of the used method for underestimating the beamspot size in the case of small statistics. In this sense the results of the 3p and 07 mid data have to be viewed critically. We expect especially σ_y to be significantly larger than the determined value. For the vertex tagging however, the precise determination of the larger σ_x is far more important than the determination of σ_y , since the latter is even below the intrinsic detector resolution. The small effect of σ_y on the total track resolution

¹For the analysis the v02 root files have been used.

²The following samples were used for MC2: v02.t3 fuy627.t1353.lfdir.0607p.jj.et4 and v02e evse26.f12583.lfdir.e2006.jj.et4; MC1 consists of the first one million events of MC2.

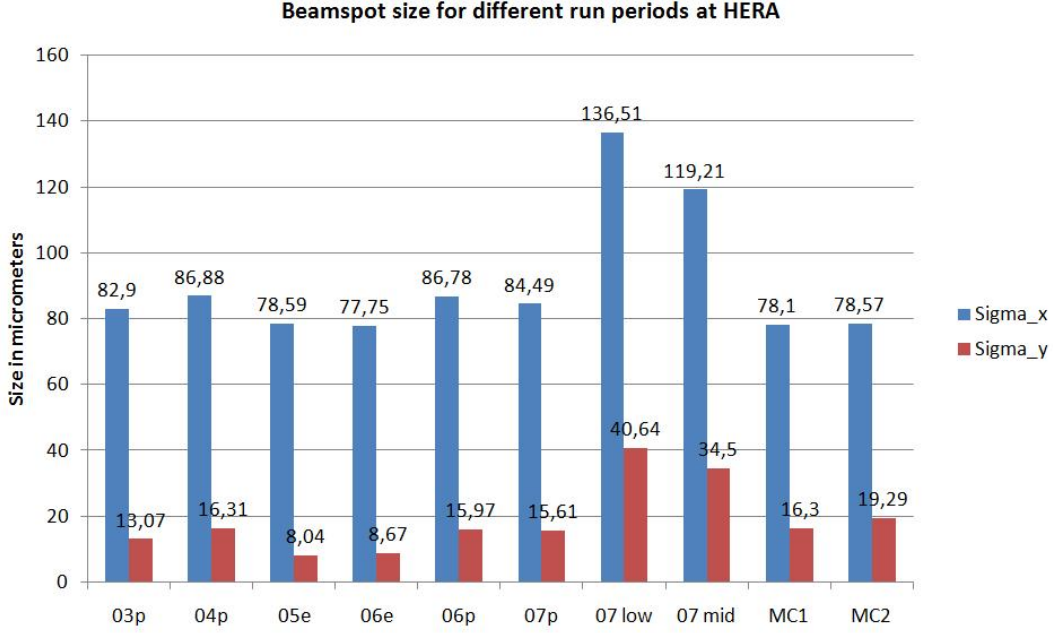


Figure 12: Beamspot size for the different run periods at HERA between 2003 and 2007

is confirmed in section 4.3.1. But even so, the σ_y value is indeed smaller than expected. Further studies need to estimate the systematic errors in this analysis in order to obtain a more realistic value for σ_y .

The interesting points to notice are that in general the beamspot is smaller for runs with electrons than for runs with positrons. This was expected ([3]) since there is an additional focusing effect for electrons through the arrangement of the bending and focusing magnets in the accelerator. Similarly, it was expected that at half the energy we would have twice the beamspot size, which was seen in the 07 low energy run with a proton energy of 460 GeV. The 07 mid run was done at an intermediate energy (with $E_{\text{proton}} = 575$ GeV), resulting in an intermediate beamspot size ([4]).

4 Multiple Scattering and Intrinsic Resolution

4.1 Resolution of the impact parameter in different scenarios

In figure 13 we have plotted the number of tracks with a certain IP versus the magnitude of the IP for a fixed ϕ with $0 < \phi < 20$ and fixed p_t with $2\text{GeV} < p_t < 2.25\text{GeV}$. It turns out that the IP distribution can be very well approximated by a Gaussian function. The mean value of the IP distribution should be, with the sign convention used for this study, identically 0. In order to get a feeling for how much the impact parameter deviates from the mean value, on average, we use the standard deviation σ_{IP} of the Gauss distribution. What is the contribution of each of the three effects described in section 2 on σ_{IP} ?

Switch off the contributions due to the beamspot size and due to the intrinsic resolution. Only multiple scattering is at work. From theory ([1]) we expect a dependence of the form:

$$\sigma_{IP} = \sigma_{\text{MultipleScatt}} = \frac{\text{const}}{p_t}$$

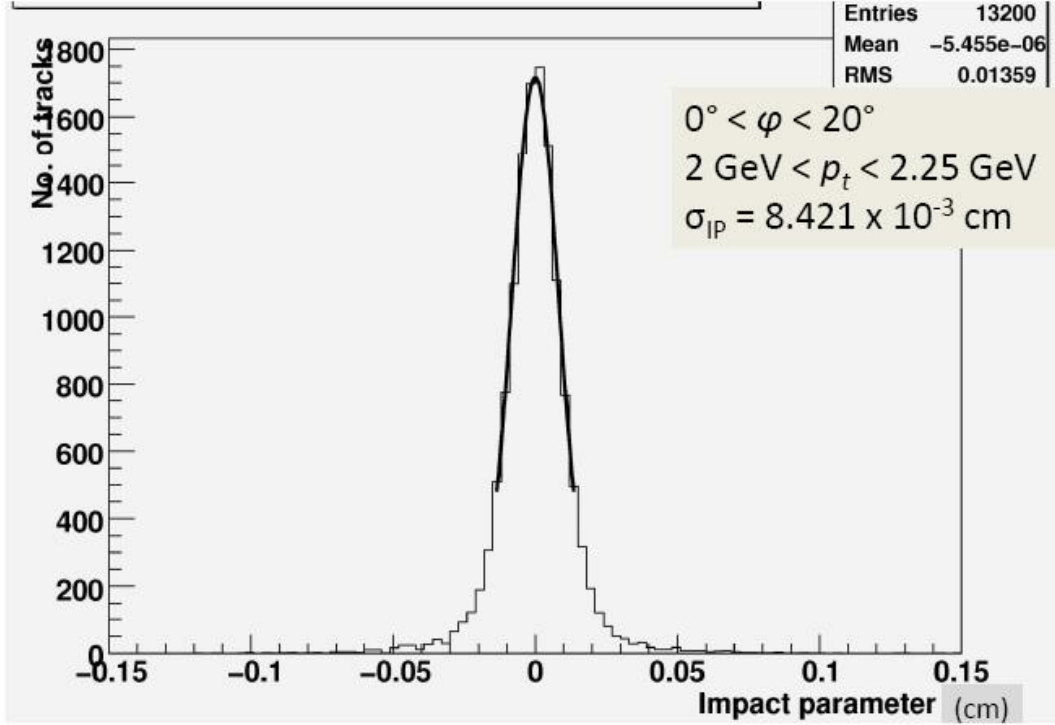


Figure 13: Number of tracks vs. IP for fixed transverse momentum p_t and ϕ angle

The constant depends on the beam pipe and detector geometry (i.e. is ϕ – dependent). This is due to the fact that in different directions a particle may see different thicknesses of the beampipe, thus being more or less victim of the scattering process.

Similarly, in the scenario in which the beamspot size effect and multiple scattering are switched off, we expect σ_{IP} to be equal to a constant term σ_{IR} due to the intrinsic resolution of detector. That is, a constant with respect to p_t , which might however be ϕ – dependent since the detector may be more sensitive in one direction than the other. This is indeed the case in the ZEUS MVD barrel, since on the “right hand side” (positive x - direction) there are more silicon strips installed than on the left, resulting on average in more hits and therefore a better resolution on one side.

In real life all three effects work at the same time and therefore their contributions have to be added quadratically:

$$\sigma_{IP} = \sigma_{\text{MultipleScatt}} \oplus \sigma_{\text{IntrinsicResolution}} \oplus \sigma_{\text{BeamSpot}}$$

which, written out in detail, gives:

$$\sigma_{IP}(\phi) = \sqrt{\left(\frac{a(\phi)}{p_t}\right)^2 + \sigma_{\text{Intrinsic}}^2(\phi) + \sigma_{\text{BSPOT}}^2(\phi)} \quad (2)$$

σ_{BSPOT} is also ϕ dependent as the following argument shows. For tracks flying off horizontally at $\phi = 0^\circ$ or 180° , the uncertainty introduced due to the existence of the beamspot is σ_y . Similarly, for tracks flying off vertically at $\phi = 90^\circ$ or -90° , the interaction point can be anywhere on the x - axis of the beamspot ellipse, introducing an uncertainty σ_x . For tracks at intermediate angles, the two contributions due to the x and y uncertainties have to be added quadratically:

$$\sigma_{\text{BSPOT}}^2(\phi) = \sigma_x^2 \cdot \sin^2 \phi + \sigma_y^2 \cdot \cos^2 \phi \quad (3)$$

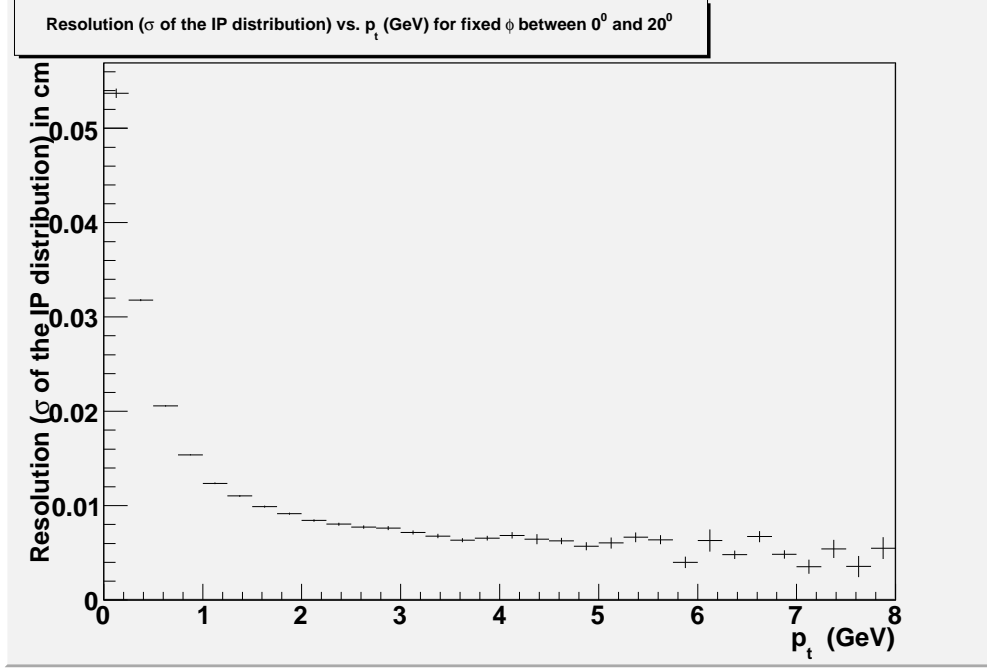


Figure 14: Total resolution (σ_{IP}) for different transverse momenta between 0 and 8 GeV at fixed ϕ

where we can use the values σ_x and σ_y determined in section 3.3. The idea now is to fit Gaussians to the distributions of number of tracks vs. IP (as in figure 13) for fixed ϕ but different p_t and plot the standard deviation σ_{IP} as a function of p_t . This has been done in figure 14.

Now we can fit a function of the form (2) to this data. By knowing σ_{BSPOT} from (3) we can extract the constants $a(\phi)$ and $\sigma_{Intrinsic}(\phi)$ for that particular ϕ out of the fit. Repeating the procedures for all ϕ bins gives complete information about the intrinsic resolution of the detector and the effect of multiple scattering for any spatial direction.

Unfortunately however, this plan fails: at small p_t the model used for multiple scattering is not appropriate due to nonlinear effects and the fit gives ambiguous results. Instead of determining $a(\phi)_{|\phi}$ and $\sigma(\phi)_{Intrinsic|\phi}$ we now fix both p_t and ϕ . Since we know $\sigma_{BSPOT}(\phi)_{|\phi}$ and we measure $\sigma_{IP|p_t,\phi}$ we can quadratically subtract the first from the second and obtain the combined effect $\sigma_{MS} \oplus \sigma_{IR}$ of multiple scattering and intrinsic detector resolution for a fixed p_t and fixed ϕ . In mathematical terms, from the measured $\sigma(\phi, p_t)_{IP|\phi, p_t}$:

$$\sigma(\phi, p_t)_{IP|\phi, p_t} = \sqrt{\sigma(\phi, p_t)_{MultipleScatt|\phi, p_t}^2 + \sigma(\phi)_{Intrinsic|\phi}^2 + \sigma(\phi)_{BSPOT|\phi}^2}$$

we obtain

$$\sigma(\phi, p_t)_{MultipleScatt|\phi, p_t} \oplus \sigma(\phi)_{Intrinsic|\phi} = \sigma(\phi, p_t)_{IP|\phi, p_t}^2 - \sigma(\phi)_{BSPOT|\phi}^2$$

which can be plotted for different angles ϕ as in figure 15.

4.2 Cuts on data

All of the 2007p data has been used for this study. We have only looked at events occuring at a primary vertex, where:

- the absolute value of the z coordinate of the vertex is < 20 cm
- there are at 10 or more tracks fitted to the same vertex

Further, we required each track to:

- have 2 or more hits in each projection in the MVD
- outer SuperLayer = 9
- $60^\circ < \theta < 120^\circ$

4.3 Results

4.3.1 Comparison of σ_{IP} and $\sigma_{MS} \oplus \sigma_{IR}$ for fixed $p_t = 5\text{GeV} \pm 10\%$ (figure 15)

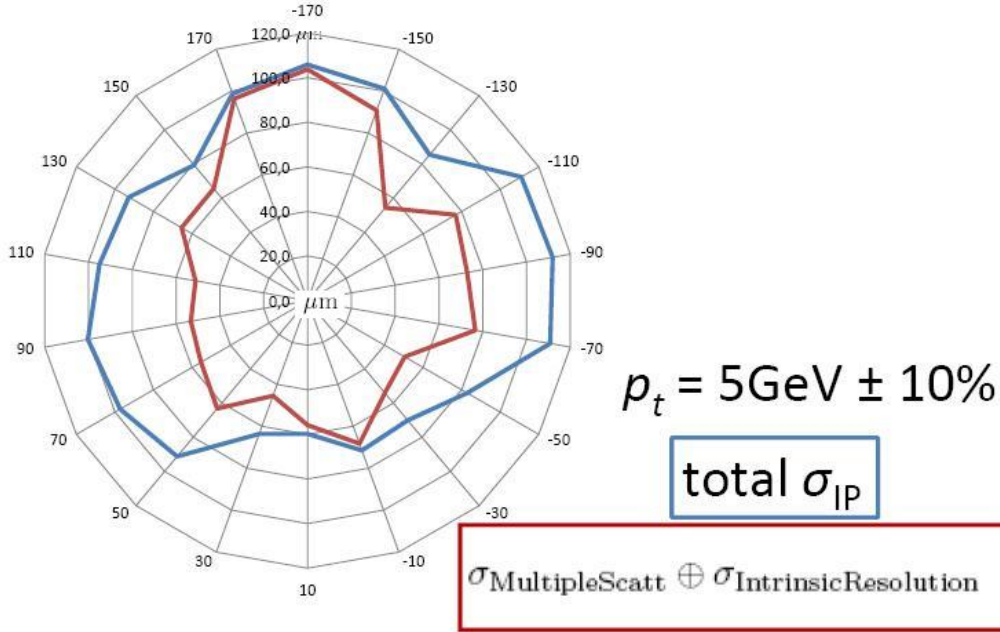


Figure 15: σ_{IP} and the quadratical subtraction of σ_{BSPOT} from σ_{IP} for $p_t = 5$ GeV

The effect of the beamspot size is clearly visible to be most important in the region $\phi = 90^\circ, -90^\circ$. Tracks flying off at these angles are perpendicular to the x -axis and thus subject to the large σ_x uncertainty on the position within the beamspot. However, this uncertainty is well understood, so when it is quadratically subtracted from the total σ_{IP} one obtains a good resolution of around 30 to 40 μm . For tracks perpendicular to the y -axis, the contribution from the beamspot to the total resolution is only σ_y , which, when subtracted quadratically, barely makes any difference.

Two points to notice: $\sigma_{MS} \oplus \sigma_{IR}$ is larger to the left (at negative x values) than to the right (at positive x -values). This is in agreement with the position of the silicon strips in the MVD

- on the left hand side there are less strips than on the right hand side, resulting in good tracks having only 2 to 3 hits in each projection on the left, but 3 to 4 hits in each projection on the right. Thus the tracks on the right hand side can be reconstructed with better precision. Secondly, the total σ_{IP} is slightly larger at $\phi = -90^\circ$ than it is at $\phi = 90^\circ$. This has to do with a shift on the y - axis of the beamspot, whose center is not quite at $y = 0$, but a few micrometers above. The silicon strips above the beamspot are closer to it and the interaction point, thus tracks can be reconstructed with better precision here.

4.3.2 Comparison of $\sigma_{MS} \oplus \sigma_{IR}$ for $p_t = 5\text{GeV} \pm 10\%$ and $p_t = 2\text{GeV} \pm 10\%$ (figure 16)

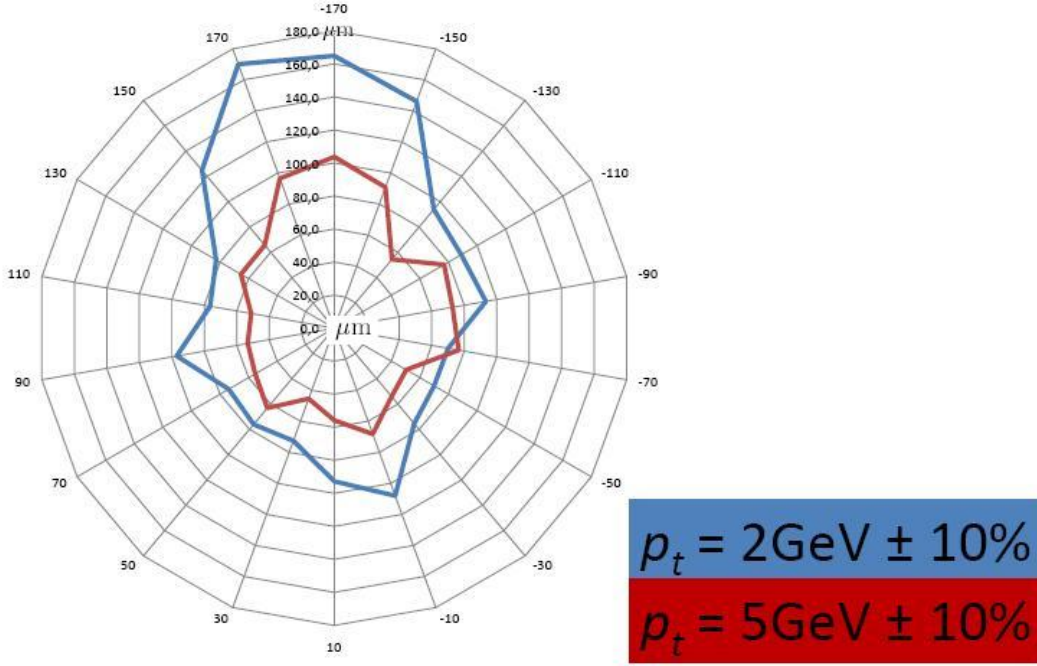


Figure 16: Effect of multiple scattering on the combined resolution $\sigma_{MS} \oplus \sigma_{IR}$ for different transverse momenta

Even though the $\frac{\text{const}}{p_t}$ model for the resolution due to multiple scattering turned out to be naive, there still is a seed of truth in it - σ_{MS} is larger, the smaller p_t is - an effect that can be seen clearly in figure 16.

4.3.3 Comparison of $\sigma_{MS} \oplus \sigma_{IR}$ for $p_t = 5\text{GeV} \pm 10\%$ for real data and Monte Carlo data (figure 17)

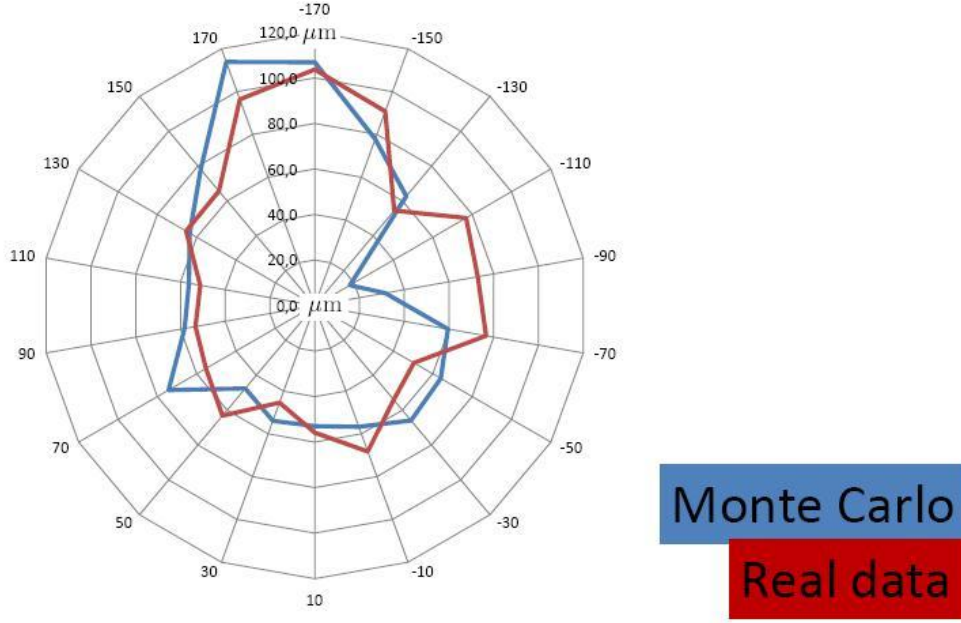


Figure 17: Track resolution $\sigma_{MS} \oplus \sigma_{IR}$ for real data and Monte Carlo data

Overall there is good agreement between MC and real data, however the Monte Carlo data gives an unusual good resolution at $\phi = 100^\circ$. This might just be a problem due to statistics.

Of course, the above analyses can be repeated for any p_t .

5 Conclusions

Through this study we have achieved a better understanding of the track quality at ZEUS:

- we performed a precision determination of the beam spot size at ZEUS for the period 2003 – 2007
- we found out that the $\frac{a(\phi)}{p_t}$ model for multiple scattering is naive; there are non-linear effects for small p_t
- we performed a determination of the combined effect of *multiple scattering* and *intrinsic detector resolution* on the impact parameter at different p_t as a function of ϕ

Further studies are desirable in order to clarify a number of issues. It is not clear what the systematic errors are when determining the beamspot size - one would like to know in how far the small values obtained for σ_y are realistic. It would be sensational if it turned out that σ_y was indeed only around $10\mu\text{m}$, half the size that was known initially.

The determination of the beamspot size has been performed integratively for a whole year - investigating shorter time periods could be interesting, since even within one fill (~ 8 hours) a small variation due to the slow blow-up of the beams with time is expected.

It is believed that with enough statistics at high p_t , one would be able to find the asymptotic behaviour of the track resolution, being able to disentangle all three effects from each other and providing an independent confirmation for the intrinsic resolution of the MVD.

6 Acknowledgements

I would like to thank Olaf Behnke for his supervision and guidance during the summer student programme, for the many hours of careful, patient explanations, corrections and clarifications. This work has been pursued during the Summer Student Program at the *research facility* DESY in Hamburg, whom the author would like to thank for excellent institutional support.

List of Figures

1	Main production diagram for charm and beauty quarks in ep collisions at HERA. (diagram Olaf Behnke)	3
2	Sketch of D^+ meson production and subsequent decay in three charged particles. On the right hand side the reconstruction of such a candidate event is shown, where one can see (in the transverse plane) the tracks as they are measured in the ZEUS barrel micro vertex detector (BMVD). (diagram Olaf Behnke)	3
3	Improvement of D^+ signal through secondary vertex tagging (plots and diagram provided by Olaf Behnke, taken from the H1 analysis DESY-04-156)	4
4	Impact parameter - ideal vs. real life	5
5	Effect of multiple scattering on the impact parameter	6
6	Contributions to the track resolution (schematic diagram - Olaf Behnke)	6
7	Sketch of the beamspot	7
8	Ideal $\langle IP_1 \cdot IP_2 \rangle$ as a function of ϕ_1 and ϕ_2 for a beamspot with $\sigma_x = 80\mu\text{m}$ and $\sigma_y = 20\mu\text{m}$	8
9	$\langle IP_1 \cdot IP_2 \rangle$ for different combinations of the two angles ϕ_1 and ϕ_2 in the case of the 05e data.	8
10	Ratio $\langle IP_1 \cdot IP_2 \rangle /$ fitted function for the determination of the beamspot size	9
11	Difference between real data and the fitted function for the determination of the beamspot size	9
12	Beamspot size for the different run periods at HERA between 2003 and 2007	11
13	Number of tracks vs. IP for fixed transverse momentum p_t and ϕ angle	12
14	Total resolution (σ_{IP}) for different transverse momenta between 0 and 8 GeV at fixed ϕ	13
15	σ_{IP} and the quadratical subtraction of σ_{BSPOT} from σ_{IP} for $p_t = 5$ GeV	14
16	Effect of multiple scattering on the combined resolution $\sigma_{MS} \oplus \sigma_{IR}$ for different transverse momenta	15
17	Track resolution $\sigma_{MS} \oplus \sigma_{IR}$ for real data and Monte Carlo data	16

References

- [1] "Uncertainties in track momentum and direction, due to multiple scattering and measurement errors." - *R. L. Gluckstern*, Nucl.Instrum.Meth.24 : 381-389, 1963
- [2] "ZEUS Tracking for the HERA-II Run" - *Rainer Mankel*, Computing Seminar, 3 July 2006, DESY
- [3] discussions with *Ferdinand Willeke*, DESY
- [4] "Beam spot size for different HERA II periods" - *Olaf Behnke*, TGR meeting, 7 January 2009, DESY